SF2A 2025
A. Siebert, K. Baillié, M. Béthermin, F. Cantalloube, E. Josselin, N. Lagarde, J. Malzac, J. Richard, L. Selliez, O. Venot (eds)

EVOLUTION OF STELLAR MAGNETIC ACTIVITY: PROBING PLANET ENGULFMENT BY RED GIANTS

C. Gehan[1]

Abstract. Red giants are particularly susceptible of engulfing planets due to the dramatic expansion of their envelope, which results in a faster surface rotation and hence a higher magnetic activity. Low-mass (LM) stars ($M \leq 1.6 M_{\odot}$) reach a maximum radius at the RGB tip that is much larger than for IM stars, making them more likely to engulf planets. I here study the evolution of the active star fraction for LM versus IM stars along the low RGB. I use the S-index, a chromospheric activity indicator, using the $\mathrm{Ca_{II}}$ H&K spectral lines for $\sim$ 3000 red giants observed by LAMOST whose evolutionary stage has been identified by asteroseismology with the *Kepler* mission. I find that the fraction of active IM stars decreases along the RGB, as expected, while the fraction of active LM stars remains globally constant along the RGB. This is not explained by models of single-star evolution and is consistent with the hypothesis that LM stars host, and therefore engulf, more planets than IM stars, as predicted by the theory of planet formation. Characterizing planet engulfment by red giants provides insights into the evolution and fate of most planetary systems, since $\sim$97% of stars pass through the red giant evolution stage.

Keywords: Asteroseismology - Methods: data analysis - Techniques: spectroscopy - Stars: activity - Stars: low-mass - Stars: planet engulfment

1 Introduction

Planets orbiting red giants allow us to study how stellar evolution impacts the orbital and physical properties of planetary systems, which is one of the main scientific goals of the future PLATO mission (ESA, 2026, Rauer et al. 2025). Additionally, planets around red giants are crucial to reach a global understanding of the survival and fate of planets, since $\sim$ 97% of stars pass through the red giant phase. Red giants are particularly susceptible of engulfing planets because their envelope dramatically expands, which accelerates the red giant surface rotation under angular momentum conservation of the star-planet system. This results in a more efficient dynamo and hence in stronger magnetic fields (Aurière et al. 2015; Privitera et al. 2016a,b). Gaulme et al. (2020) have measured the fractions of magnetically active red giants exhibiting spots in co-rotation with their photosphere by analyzing *Kepler* light curves, for different mass intervals and for two distinct evolution stages: the red giant branch (RGB) where stars burn hydrogen in a shell around the inert helium core, and the more evolved horizontal branch (HB) where stars undergo core-helium burning. Gaulme et al. (2020) found that the fraction of spotted intermediate-mass (IM) stars ($M > 1.5\, M_{\odot}$) decreases between the RGB and the HB, as expected. However, the fraction of spotted low-mass (LM) unexpectedly increases between the RGB and the HB, which Gaulme et al. (2020) interpreted as a potential signature of planet engulfment by these stars. This hypothesis is reinforced by the fact that models predict that the maximal radius reached at the tip of the RGB is much larger for LM stars than for IM stars, making them more susceptible of engulfing planets along the RGB. In order to check this hypothesis further, we need to study the evolution of the active star fraction along the RGB and not only between the RGB and the HB as was done by Gaulme et al. (2020). However, the photometric detection of photospheric spots is subject to biases towards large and/or long-living spots (Rackham et al. 2018; Basri & Shah 2020), which can in turn bias the active star fractions measured from spot detection. In order to obtain a more complete view of the evolution of red giants magnetic activity, we need independent activity indicators, regardless of whether or not spots are detected.

[1] IRAP, Université de Toulouse, CNRS, CNES, UPS, 14 avenue Edouard Belin, 31400 Toulouse, France

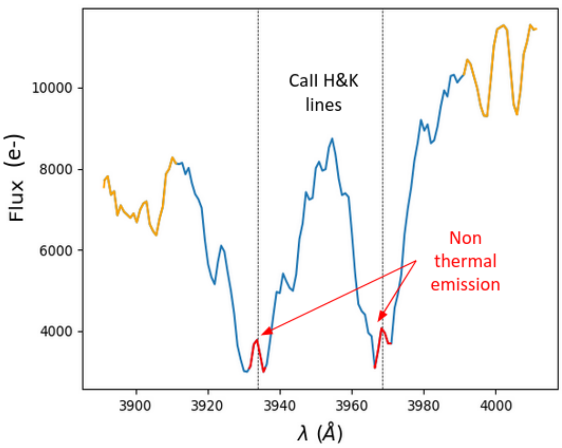

Fig. 1. $\mathrm{Ca_{II}}$ H&K lines for a red giant observed by LAMOST (DR7). The wavelength range used to compute F_H and F_K is highlighted in red while the wavelength range used to compute F_B and F_R is highlighted in orange. The location of the line centers is represented by the vertical lines.

2 Method and Data

I considered the spectroscopic S-index, which measures the magnetic activity level in the chromosphere of cool stars and is a proxy of the strength of surface magnetic fields (Babcock 1961). Magnetic fields generate a non-thermal heating of the chromosphere, which results in excess emission with respect to a radiative equilibrium atmosphere in the center of some absorption lines, among which the $\mathrm{Ca_{II}}$ H&K lines at 3969 and 3934 Å respectively (Hall 2008, and Fig. 1). The S-index essentially measures the depth of these lines such that (Wilson 1978; Duncan et al. 1991)

$$S_{\mathrm{Ca_{II}\,H\&K}} = \frac{F_H + F_K}{F_B + F_R}, \tag{2.1}$$

where F_H and F_K correspond to the integrated flux in the center of the H and K lines, respectively (in red in Fig. 1), while F_B and F_R correspond to the integrated flux in the blue and red pseudo-continuum nearby (in orange in Fig. 1). I used data from the Large Sky Area Multi-Object Fibre Spectroscopic Telescope (LAMOST, DR7) because, although is has a low spectral resolution ($R = 1600$), millions of spectra are available for cool stars that include many red giants observed by the *Kepler* mission, for which we know the evolutionary status (RGB versus HB) thanks to asteroseismology. I focused on the sample of $\sim$ 4400 red giants analyzed by Gaulme et al. (2020), which have $4 < R < 15\,R_\odot$ in order to discard subgiants as well as red giants too evolved to unambiguously identify their evolution stage (Dupret et al. 2009; Grosjean et al. 2014; Dréau et al. 2021).

3 Properties of stellar evolution and of known exoplanets

On the one hand, surface rotation is expected to slow down as R^{-2} due to the envelope expansion. I computed models with different masses with the MESA stellar evolution code (Paxton et al. 2011), which indicate that the radius expands at the same rate along the RGB (left panel of Fig. 2). Additionally, models indicate that mass loss remains negligible, below 2%, on the low RGB considered here ($R < 15\,R_\odot$). Therefore, we expect the surface rotation and hence magnetic activity to evolve similarly for stars with different masses along the RGB, in the absence of planet engulfment or other external interactions.

On the other hand, the great majority of the known planets are orbiting LM stars (right panel of Fig. 2). This partly reflects an observational bias but the theory of planet formation nevertheless supports this observation as it predicts that the number of formed planets is largely determined by the lifetime of the protoplanetary disk (Ronco et al. 2017; Guilera et al. 2020; Venturini & Helled 2020; Venturini et al. 2020), which decreases with stellar mass (Ribas et al. 2015; Kunitomo et al. 2021; Ronco et al. 2024). IM stars thus have less time to form planets and therefore form less planets. Moreover, we already expect LM stars to engulf planets on the low RGB considered here ($R < 15\,R_\odot$, see the magenta crosses in the right panel of Fig. 2). Hence, we expect magnetic activity to evolve differently for LM and IM stars along the RGB because of planet engulfment.

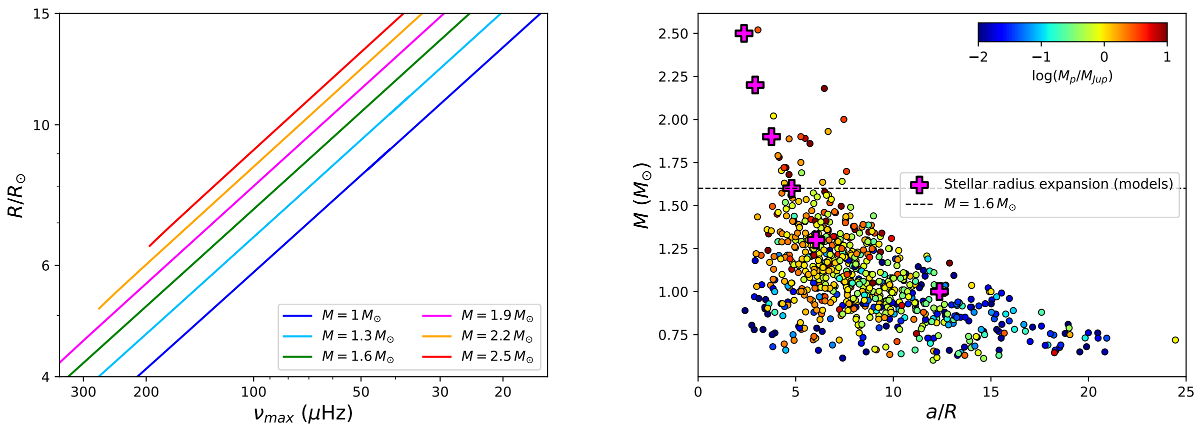

Fig. 2. Properties of stellar evolution and of known exoplanets. *Left:* Evolution of the stellar radius on the low RGB for models with different masses computed with the MESA evolution code, from $R = 4\,R_\odot$ up to $R = 15\,R_\odot$ that is the maximum radius in the studied observational sample, as a function of the asteroseismic parameter $\nu_{\rm max}$ (in log scale, inverted axis) tracing the degree of evolution along the RGB. *Right:* Mass of main-sequence stars ($R \leq 4\,R_\odot$) known to host planets as a function of the ratio between the semi-major axis of the planet and the stellar radius. The color code represents the decimal logarithm of the planets mass, in Jupiter masses. The horizontal dashed lines indicate a mass of $M = 1.6\,M_\odot$. The magenta crosses indicate the ratio between $R = 15\,R_\odot$ on the RGB and the radius at the end of the main sequence, for the models shown on the left-hand panel.

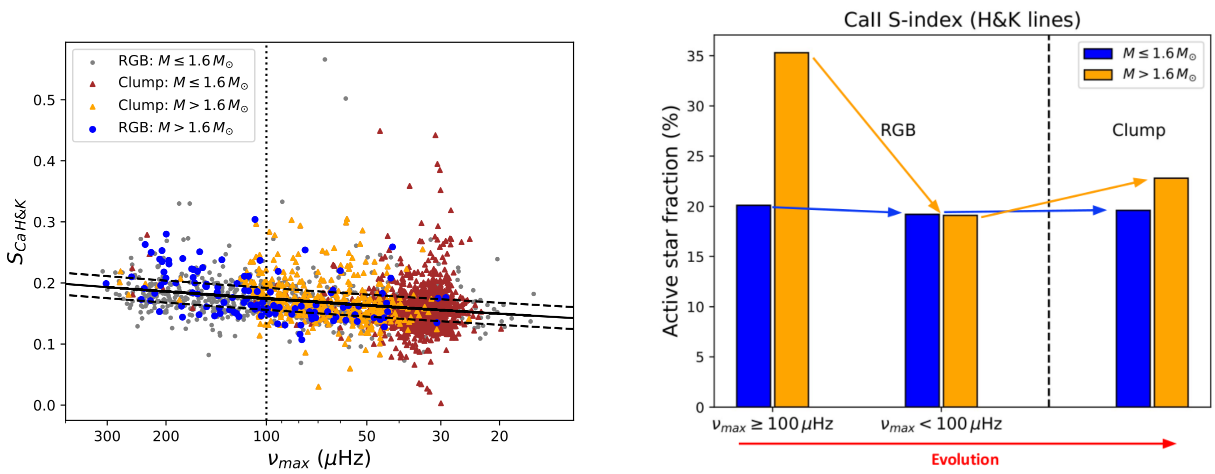

Fig. 3. Results. *Left:* S-index as a function of $\nu_{\rm max}$ (inverted axis), hence of evolution. LM and IM stars on the RGB are represented by grey and blue dots, respectively. LM and IM stars on the HB are represented by red and orange triangles, respectively. The vertical dotted lines indicate $\nu_{\rm max} = 100\,\mu$Hz. The continuous and dashed lines represent a fit by a power law to the RGB stars and the corresponding 5-σ uncertainty, respectively. *Right:*. Active star fractions for LM and IM stars along the RGB and on the HB (indicated as Clump in the figure).

4 Results

I measured the S-index of $\sim$ 3000 RGB and HB stars (Gehan et al. 2022, 2024, left panel of Fig. 3). I discriminated between LM ($M \leq 1.6 M_\odot$) and IM ($M > 1.6 M_\odot$) stars on the RGB and the HB, and I also considered separately less evolved from more evolved stars on the RGB, separated by $\nu_{\rm max} = 100\,\mu$Hz. I computed the active star fractions as the fraction of stars that have a S-index above the fit corresponding to the average activity level along evolution, plus its 5-σ uncertainty (upper dashed lines in the left panel of Fig. 3).

The active star fraction along the RGB decreases for IM stars as expected, but remains globally constant for LM stars (right panel of Fig. 3), which is consistent with the hypothesis that LM stars engulf more planets than IM stars. Between the RGB and the HB, on the contrary, the active star fraction increases for IM stars while still remaining globally constant for LM stars. However, this is not necessarily inconsistent with the fact that LM stars engulf more planets since mass loss comes into play for those more evolved stars. Models indicate that the fraction of mass that is lost at the tip of the RGB with the Reimers prescription (Reimers 1975) is much more important for LM stars than for IM stars, contributing in making LM stars less active on the HB. Hence, the results are less straightforward to interpret than along the RGB.

We can wonder if these results cannot be explained by tidal interactions with a stellar companion instead of planet engulfment. The stars I analyzed are single red giants that have not been identified as belonging to multiple stellar systems by the *Gaia* mission (DR3). Moreover, the fraction of multiple stellar systems increases with the mass of the primary star (Whitworth & Lomax 2015; Moe & Di Stefano 2017), which is not compatible with the observational indication that LM red giants engulf more companions than IM red giants. Hence, a scenario of stellar merger seems to be excluded to explain the current results.

5 Conclusions

The evolution of the active star fraction along the RGB is compatible with the hypothesis that LM stars ($M \leq 1.6M_{\odot}$) engulf more planets than IM stars ($M > 1.6M_{\odot}$). Additionally, the evolution of the active star fraction from the RGB (shell-H burning stage) to the HB (core-He burning phase) is not necessarily inconsistent with more planets being engulfed by LM stars because mass loss comes into play for these more evolved stars, making the results less straightforward to interpret than along the RGB. The future PLATO (ESA, 2026) mission is expected to observe more than 10 000 red giants within the Science Calibration and Validation program, which will open new perspectives for the emerging field of the study of planet engulfment by evolved stars.

C. G. was supported by a postdoctoral fellowship from the CNES, and warmly thanks P. Gaulme for fruitful discussions.

References

Aurière, M., Konstantinova-Antova, R., Charbonnel, C., et al. 2015, A&A, 574, A90
Babcock, H. W. 1961, ApJ, 133, 572
Basri, G. & Shah, R. 2020, ApJ, 901, 14
Dréau, G., Mosser, B., Lebreton, Y., Gehan, C., & Kallinger, T. 2021, A&A, 650, A115
Duncan, D. K., Vaughan, A. H., Wilson, O. C., et al. 1991, ApJS, 76, 383
Dupret, M. A., Belkacem, K., Samadi, R., et al. 2009, A&A, 506, 57
Gaulme, P., Jackiewicz, J., Spada, F., et al. 2020, A&A, 639, A63
Gehan, C., Gaulme, P., & Yu, J. 2022, A&A, 668, A116
Gehan, C., Godoy-Rivera, D., & Gaulme, P. 2024, A&A, 686, A93
Grosjean, M., Dupret, M. A., Belkacem, K., et al. 2014, A&A, 572, A11
Guilera, O. M., Sándor, Z., Ronco, M. P., Venturini, J., & Miller Bertolami, M. M. 2020, A&A, 642, A140
Hall, J. C. 2008, Living Reviews in Solar Physics, 5, 2
Kunitomo, M., Ida, S., Takeuchi, T., et al. 2021, ApJ, 909, 109
Moe, M. & Di Stefano, R. 2017, ApJS, 230, 15
Paxton, B., Bildsten, L., Dotter, A., et al. 2011, ApJS, 192, 3
Privitera, G., Meynet, G., Eggenberger, P., et al. 2016a, A&A, 593, L15
Privitera, G., Meynet, G., Eggenberger, P., et al. 2016b, A&A, 593, A128
Rackham, B. V., Apai, D., & Giampapa, M. S. 2018, ApJ, 853, 122
Rauer, H., Aerts, C., Cabrera, J., et al. 2025, Experimental Astronomy, 59, 26
Reimers, D. 1975, Memoires of the Societe Royale des Sciences de Liege, 369
Ribas, Á., Bouy, H., & Merín, B. 2015, A&A, 576, A52
Ronco, M. P., Guilera, O. M., & de Elía, G. C. 2017, MNRAS, 471, 2753
Ronco, M. P., Schreiber, M. R., Villaver, E., Guilera, O. M., & Miller Bertolami, M. M. 2024, A&A, 682, A155
Venturini, J., Guilera, O. M., Ronco, M. P., & Mordasini, C. 2020, A&A, 644, A174
Venturini, J. & Helled, R. 2020, A&A, 634, A31
Whitworth, A. P. & Lomax, O. 2015, MNRAS, 448, 1761
Wilson, O. C. 1978, ApJ, 226, 379